Optimization of 100 µm alginate-Poly-L-Lysine-alginate capsules for intravitreous administration.

Authors: **E. Santos[1,2], G. Orive[1,2], A. Calvo[3], R. Catena[3], P. Fernández-Robredo[4], A. García Layana[4], R.M. Hernández[1,2], J.L. Pedraz[1,2]**

[1]NanoBioCel Group, Laboratory of Pharmaceutics, University of the Basque Country, School of Pharmacy, Vitoria, Spain; [2]Biomedical Research Networking Center in Bioengineering, Biomaterials and Nanomedicine (CIBER-BBN), Vitoria, Spain.

[3]Laboratory of Novel Therapeutic Targets, Centre for Applied Biomedical Research (CIMA), University of Navarra. Avenida Pío XII 57, 31007 Pamplona, Spain.

[4]Departamento Oftalmología. Clínica Universidad de Navarra, Pamplona,

Corresponding Author: José Luis Pedraz (joseluis.pedraz@ehu.es)
Laboratory of Pharmaceutics, University of the Basque Country, School of Pharmacy, Vitoria, Spain

Keywords: APA, microcapsule, alginate, Flow Focusing, Central Nervous Disease, reduced size, intravitreous

Running title: Small-sized alginate-poly-L-lysine-alginate capsules for intravitreous administration.

ABSTRACT

The field of cell microencapsulation is advancing rapidly. Particle size plays a critical role in terms of biocompatibility and limits decisively its applicability. Producing reduced size microcapsules involves broadening the possibilities to employ this technology in the treatment of many disorders. Nervous system diseases (NDS) represent a clear example of that. This work describes the feasibility of reducing the size of alginate-poly-L-lysine-alginate (APA) microcapsules up to 100 μm in a highly monodisperse way using the novel *Flow Focusing* technique. C_2C_{12} myoblasts genetically engineered to express the triple reporter gene thymidine kinase-green fluorescent protein-luciferase (TGL) and secrete vascular endothelial growth factor soluble receptor 2 (VEGFR2, also known as KDR) were encapsulated for further characterization. Resulting new particles were assayed *in vitro* to explore whether their functionality might be affected due to the physicochemical changes arising from such dramatic size reduction. Not only no negative effects at this level were noticed in terms of cell viability, cell proliferation and KDR secretion, but once again the suitability of APA microcapsules was reinforced against other microcapsule designs. Furthermore, the fully viable and functional biosystems were successfully administered in the intravitreous space of rats, where the activity of encapsulated cells was monitoring over 3 weeks.

INTRODUCTION

In the era where drug delivery represents an important limiting factor for the achievement of successful therapies in many diseases, cell-based drug delivery approaches emerge as promising alternatives [1]. In particular, in cell microencapsulation technology, cells may act as customized factories producing the desired therapeutic factor *de novo* and in a sustained way. This is of a remarkable importance, first due to the biological and physicochemical properties that proteins must conserve in order to maintain their activity, and second because it avoids the use of repeated shots [2]. In the last few years, cell microencapsulation technology is gaining progressively the interest of the scientific community [3,4]. To date, this technology has rendered multiple improvements in order to meet the requirements needed to take the step to clinical practice [5]. From diabetes to cancer, numerous therapies have been already tested in clinical trials using cell microencapsulation technology [6-9].

However, when it comes to deal with the treatment of Central Nervous System (CNS) diseases and eye disorders, reducing particle size represents a major challenge [10]. In fact, small-sized microcapsules have been demonstrated to show increased mechanical properties, better relation surface/volume, reduced mass transport limitations, and enhanced biocompatibility [11,12]. In addition, for cell-therapies that need a rapid stimuli response in a concentration- and time-dependent way, diameter reduction translates into faster diffusion of the molecules to the center of the device and into a faster therapeutic response [13,14]. However, several important challenges exist when developing these small-sized cell-loaded devices. Determining the minimal cell load necessary to obtain a 100% encapsulation yield, evaluating cell viability changes that may occur as a result of possible permeability and physicochemical changes arising from such dramatic size reduction and optimizing the maximum capsule load (dose) within the smaller administration volume are only some few examples.

In the search of achieving such small particle size, the necessity for moving from the established technologies has increased. In this sense, the classic electrostatic droplet generator, while still suitable for standard 300-500 μm beads, is starting to fall behind if ≤200 μm particle size is intended [15,16]. Other techniques such as vibrating nozzle or Jet Cutter® have also demonstrated to be unable to reproduce efficiently cell entrapping particles below this threshold [17-19]. More promising results have been obtained using air co-axial flow technique, by which generation of 100-200 μm alginate-poly-L-lysine-alginate (APA) capsules has been reported [11,19,20]. However, capsules obtained with this procedure still need further improvements in terms of uniformity and morphology. Using microfluidic technologies highly homogeneous beads of sub-sieving size (<100 μm) have been produced [21], although it remains to be determined whether this technology can be fully used in the field cell microencapsulation. The *Flow Focusing System* represents an appealing alternative to fabricate small-sized particles as it provides the same mild conditions than traditional droplet generators, but it improves intra and inter capsule batch reproducibility. Moreover, it is straightforward to scale-up and maintain under aseptic conditions [22,23].

Retinal diseases are the leading cause of legal blindness in developed countries. Among these pathologies age macular degeneration (AMD) and diabetic macular edema (DME) are the most prevalent in people older than 55 years old [24]. Vascular endothelial growth factor (VEGF) is an important angiogenic cytokine in normal and pathological processes such as choroidal neovascularisation (CNV; characteristic process of the wet form of AMD) [25]. The intraocular release of therapeutic agents that inhibit VEGF action has a great potential for the treatment of chronic retinal diseases,

such as AMD and DME. Flk-1/KDR, the soluble form of VEGF receptor, and ranibizumab, a monoclonal anti-VEGF antibody, represent two of the most promising options for this treatment [26]. However, the need of monthly intravitreal injections is the main disadvantage of the current treatment with a high discomfort for the patient and an overcharge of work for the health systems [27,28]. Retina shows a unique microenvironment in which a higher metabolic ratio succeeds together with hematorretinal barrier and particular anatomy of the eye. These conditions make the retina an unavailable tissue for therapeutic molecules. The immobilisation of cells genetically modified to produce these antiangiogenic molecules is particularly attractive in the treatment of those chronic pathologies which require continuous and controlled administration of therapeutic products in the long term, since one administration ensures the effectiveness of treatment for several months.

The objective of the present study is to encapsulate murine C_2C_{12} cells, genetically engineered to express both the triple reporter gene thymidine kinase-green fluorescent protein-luciferase (TGL) and KDR within 100 µm APA microcapsules by means of the *Flow Focusing System*, with the aim of tackling a future retinopathy model in rats. In vitro and in vivo functionality and viability of encapsulated cells was analyzed. Furthermore, a detailed evaluation of the fabrication and characterization processes has been carried out in order to guarantee particle uniformity, reproducibility, optimum cell viability and successful implantation. To our knowledge, this is the first time such particle size is achieved with APA capsules in monodisperse batches and, those beads are implanted successfully in intravitreous space in vivo.

MATERIAL AND METHODS

Cell culture

Murine C_2C_{12} myoblasts derived from the skeletal muscle of an adult C3H mouse and genetically engineered to express the triple reporter gene TGL and secrete KDR were grown in Dulbecco's modified Eagle medium (DMEM) supplemented with 10% fetal bovine serum (FBS), L-glutamine to a final concentration of 2 mM, 4.5 g/L glucose, 1% antibiotic/antimycotic solution and 2.5 ug/mL Blasticidin selection antibiotic (Invivogen). Cultures were plated in T-flasks, maintained at 37 °C in a humidified 5% CO2/95% air atmosphere standard incubator, and were passaged every 2-3 days. All reagents were purchased from Gibco BRL (Invitrogen S.A., Spain).

Generation of KDR secreting triple reporter C_2C_{12} myoblasts (C_2C_{12}-TGL-KDR)

Transduction of the C_2C_{12} myoblasts with the $pSFG_{NES}TGL$ retrovector (kindly provided by Dr. Ponomarev [29], Memorial Sloan Kettering Cancer Center, NY) to generate the triple reporter C_2C_{12} myoblasts (C_2C_{12}-TGL) has been recently described by our group [30]. This clone was further transfected with the episomic plasmid pBLAST-sFlk-1 (Invivogen) to secrete the VEGF soluble receptor KDR. Transfection was carried out using the lipofectamine 200 method (Invitrogen) according to manufacturer's indications with 5 ug of the plasmid pBLAST-sFlk-1 (Invivogen). 36 hours after transfection, cells were treated with 5 ug/mL Blasticidin during a period of

one week to allow for selection. Resistant clones were pooled and maintained in Blasticidin selection to avoid plasmid loss.

Cell microencapsulation

C_2C_{12} myoblasts genetically engineered to express the triple reporter gene TGL and to secrete KDR were encapsulated into APA microcapsules using *Flow Focusing System* (Ingeniatrics Tecnologías, S.L.) and following a brief modification of Lim & Sun's procedure [31]. Ultra pure low-viscosity high glucuronic acid alginate (UPLVG) was purchased from FMC Biopolymer, Norway. Poly-*L*-lysine (PLL hidrobromide M_w 15 000–30 000 Da) was obtained from Sigma Aldrich (St. Louis, MO, USA). Briefly, cells were harvested from monolayer cultures using trypsin-EDTA (Invitrogen), filtered through a 40 µm pore mesh and resuspended in 1.5% sodium alginate at varying densities (2×10^6, 5×10^6 and 10×10^6cells/mL). The resulted suspension was extruded in a sterile syringe through a 0.24 mm diameter nozzle tip (orifice diameter) at a flow rate of 2 ml/h using a peristaltic pump, and focused with sterile air at 90 to 120 mbar pressure. The drops were collected in a 55 mM $CaCl_2$ solution and maintained in a shaker after the end of the process for 15 min in order to ensure complete gelification of all the particles. Subsequently, the beads were suspended in 0.05% PLL solution for 5 min, washed twice with 10 mL of manitol 1% and coated again with another layer of 0.1% alginate for 5 min. Finally, microcapsules were cultured in complete medium. The whole process was carried out at room temperature and under aseptic conditions. For in vitro assays, obtained particles were subdivided into 3 subgroups. One group was kept uncoated, other group was coated to form APA capsules, and the third group was coated and further core liquefied with 1% citrate solution. For in vivo assays APA capsules were employed.

Cell viability and encapsulation yield assessment

Cells within the particles were dyed with the LIVE/DEAD kit (Invitrogen) and after 30 min, fluorescence micrographies were taken with an epi-fluorescence microscope (Nikon TSM). Analyses of ten randomly taken images per group were performed to quantify the number of empty capsules and the number of capsules enclosing no one living cell (dead capsules).

Quantification of cell metabolic activity.

Metabolic activity was determined on the basis of tetrazolium production using the Cell Counting Kit-8 (CCK-8) (Dojindo). Briefly, 100 µL of capsule suspension (2000 capsule ≈ 10000 cells) was inoculated per well in a 96-well plate. 10 µL of CCK-8 were added to each well and after 4 h incubation at 37ºC, colour development was read at 450 nm. All values were corrected with the reference wavelength at 690 nm and normalized against the mean value of 3 blank wells (medium) for each experiment. Results are shown as mean of 7 independent samples ± S.D per study group.

Measurement of KDR secretion

Cell supernatants were assayed for KDR secretion using the Quantikine IVD Human sVEGF R2/KDR/Flk-1 ELISA Kit purchased from R&D Systems (Minneapolis, MN). Standards and samples were run in duplicate according to the procedure specified in the kit. The KDR secretion of 10,000 capsules/mL (the equivalent of 50,000 cells/mL) was measured for a 24 h release period in triplicate per study group. Results are expressed as mean ± S.D.

Cell proliferation assay

The equivalent of 2 x 10^4 cells/100 µL (≈ 4000 microcapsule/well) was placed into each well of 96-well plate. All groups were incubated with complete medium supplemented with 10% FBS except the negative control group, which was incubated with starving medium supplemented with 0.1% FBS. After 24 h, the encapsulated cells were incubated in the presence of 10 µM BrdU for additional 24 h. Then, cells were de-encapsulating with a solution of medium containing 500 µg/mL of alginate lyase (Sigma-Aldrich) and assayed for BrdU uptake using Cell Proliferation Biotrak ELISA System (Amersham, NJ, USA) following manufacturer's indications. Absorbances of the non-specific binding control group (without BrdU) were subtracted from the rest of the groups, and results were normalized with the corresponding negative control for each experiment. Data are shown as mean of 5 independent samples ± S.D per study group.

Administration of cell-loaded microcapsules

100 µL capsules were pelleted in a 1.5 mL tube using a Sprout® Mini-Centrifuge and 10 µL doses were loaded directly aspirating from that pellet with a high-precision Hamilton syringe (Gastight 1702LT Hamilton Co., Reno, NV) connected to 25G, 27G and 30G needles. Total number of microcapsules per shot was counted employing an inverted optical microscopy. Results represent the mean of 6 shots ± S.D for any needle size.

Animals and implantation surgery

For *in vivo* studies 3 adult Wistar rats (Harlan) were intraperitoneally anesthetized with a mixture of ketamine (Imalgene 1000) (75 mg/kg) and Xylacine (Rompun 2%) (10 mg/kg). Injections were performed with a 1 mL syringe and a 25-gauge needle. Intravitreal injections were performed with high-precision Hamilton syringes (Gastight 1702LT Hamilton Co., Reno, NV) and peribulbar 25G canule. Injection site was located 1 mm posterior to the corneoscleral limbus. A single 10 µl injection of microencapsuled cells was administered in the treated eye (left) and the same volume of vehicle solution in the contralateral eye (right, intravitreal controls).

Retinographies and detection of luciferase activity

Microcapsules were dyed with Membrane Blue before administration and pictures were taken using a Canon® CF-60 ZA Retinograph. D-Luciferin (300 µg in 10 µL volume) was administered to the rats under anaesthesia by intravitreal injection every week after capsule inoculation and the emission of photons was measured in Xenogen IVIS 100 series luminometer living image system (Caliper Life Scieces, Hopkinton, MA).

Statistical analysis

Data are presented as mean ± S.D. All statistical computations were performed using SPSS 18.0 (SPSS, Inc., Chicago, IL). Student's t-test was used to detect significant differences when two groups were compared. One-way ANOVA and post-hoc test were used in multiple comparisons. The Bonferroni, or Tamhane post-hoc test was applied according to the result of the Levene test of homogeneity of variances.

RESULTS

Production of 100 µm diameter APA microcapsules and optimization of the cell load to ensure high encapsulation yield

100 µm diameter microcapsules were obtained using the *Flow Focusing System*. The pressure of focusing air jet range from 90 to 120 mbar as cell density in the pre-gelled solution was increased. All particles showed perfect spherical shape with smooth surface with no irregularities and a narrow size distribution of less than 10% CV. A negligible percentage of broken or defective capsules was observed (Fig 1).

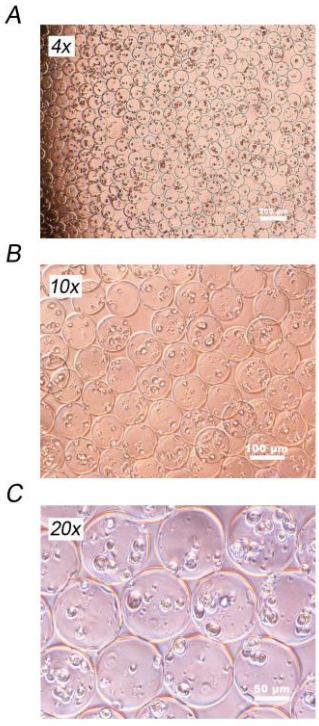

Figure 1

Probabilities for the occurrence of empty capsules adjusted to the mathematical model of Poisson's Distribution as determined after analyzing the correlation of theoretical and experimental data (Fig. 2 A-B). Microcapsules bearing no single living cell were considered non-functional and labeled as "Dead Capsules". The presence of these microcapsules appeared in values of about 3.67% for cell loads of 10 x 10^6 cells/mL, while for lower cell loads the number of dead capsules increased dramatically, 56.3% and 68.7% for 5 x 10^6 and 2 x 10^6 cells/mL respectively (Fig 2 B-C).

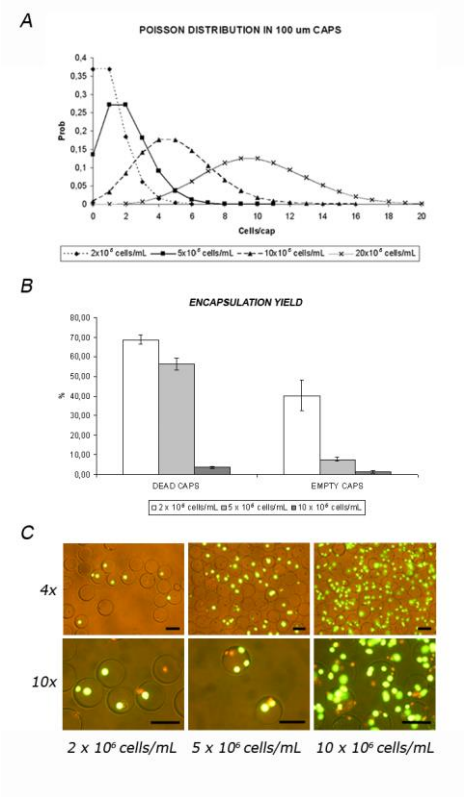

Figure 2

APA microcapsules of 100 µm diameter present suitable conditions to allow sustained high cell viability, cell proliferation and delivery of therapeutic products *in vitro*.

Three different batches of microcapsules were produced to examine the causes that might compromise the complete functionality of cells within 100 µm-sized APA microcapsules. Thus, classical APA microcapsules were assayed in parallel with liquid core microcapsules, which avoid the drawbacks that may arise due to a too stiff matrix, and uncoated beads, which avoid limitations in terms of either permeability or over exposition to the PLL polycation.

All the groups increased their metabolic activity reaching a peak by day 10 (Fig 3 A). From that point onward and after a general slight decrease, APA microcapsules maintained a high metabolic activity up to the end of the assay. The rest of the groups suffered a more pronounced and continued decay that became statistically significant with respect to the APA group from day 24 to day 31 ($p<0.01$). The liquid core

microcapsules showed the lowest metabolic activity at the end of the experiment, which also was significantly different in comparison with the uncoated group ($p<0.05$).

KDR secretion was found to attain a maximum value immediately after encapsulation of the cells (Fig 3 B). In the following weeks, secretion levels for all the groups declined by half of the initial values and tended to remain constant until the last measurement (day 31). The uncoated microcapsules underwent a slight delay in this respect, but finally matched the others groups showing no statistical significances by day 24 (with both APA and liquid core groups) and day 31 (only when comparing with APA group). Once again, liquid core microcapsules reflected the worst results at the end of the experiment, albeit the difference was only statistically significant when compared to the uncoated group.

Micrographies taken with LIVE-DEAD dye revealed an overall good appearance of the encapsulated cells, both at the beginning and the end of the study for all the groups (Fig 3 C).

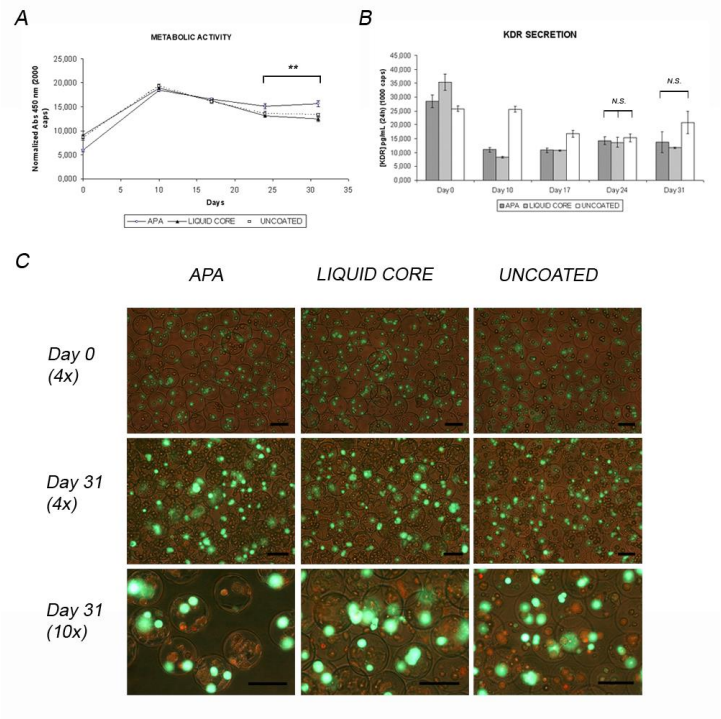

Figure 3

In addition, APA and liquid core microcapsules were assayed for DNA synthesis in order to detect possible differences in cell proliferation rates. Both types of microcapsules demonstrated a positive BrdU uptake during the experiment (Fig 4) ($p< 0.01$). APA group incorporated less pyrimidine analogue in the second week (day 12) than that found for the liquid core. By day 35, the values in the APA group had significantly increased in comparison with those taken in the first measurement ($p< 0.01$) and those obtained with the liquid core group ($p< 0.05$). These results come along with those obtained in the metabolic activity assay.

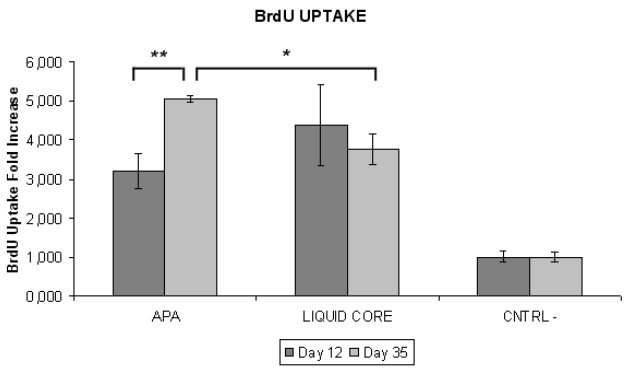

Figure 4

Entering the intravitreous space: Loading the highest number of microcapsules in the lowest possible volume.

Three different needle gauges were tried in order to load the maximum possible number of microcapsules in a 10 µL volume injection. Administration yield gave clearly the best results for 25G needles (6781 ± 1327 microcapsules/10 µL) when compared with both 27G (2958 ± 1023 microcapsules/10 µL) and 30 G needles (43 ± 18 microcapsules/10 µL) (Fig 5 A). In addition, the variability of the procedure diminished as the needle inner diameter increased: 41.3%, 34.5% and 19.5%, for 30G, 27G and 25G respectively. All the differences were statistically significant ($p < 0.05$).

The *in vivo* administration procedure was optimized in three Wistar rats (left eye in each rat) dying APA microcapsules with Membrane Blue (Fig 5 B shows a single dose of 10 µL shot) and tracking the entrance into the intravitreous space by posterior performance of retinography images (Fig 5 C).

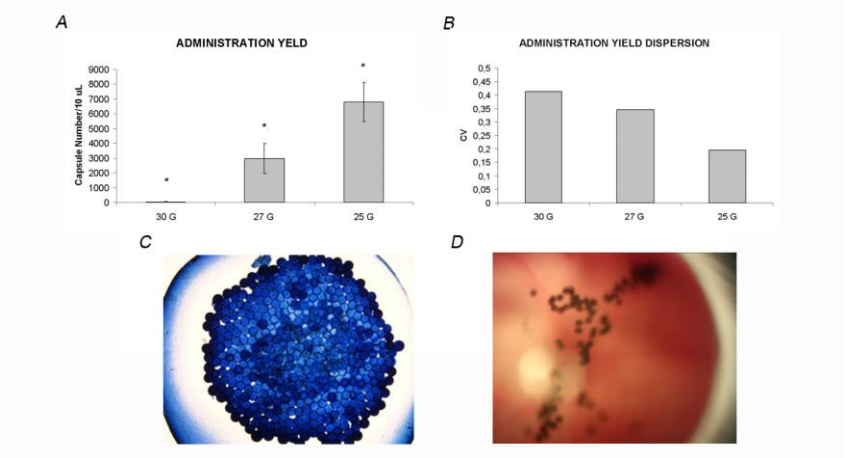

Figure 5

Encapsulated cells placed into the intravitreous space remained viable for at least 3 weeks after the implantation.

In order to ensure the applicability of small diameter APA microcapsules in the treatment of ophthalmic diseases, the viability of enclosed cells was measured over the following 3 weeks after the administration. Encapsulated C_2C_{12}-TGL cells emitted a

strong signal after D-Luciferin injection (Fig 6 A-C), illustrating that en enclosed cells remained viable within the small diameter microcapsules.

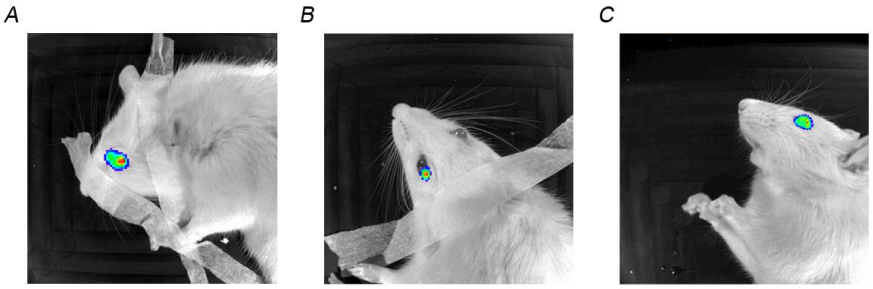

Figure 6

DISCUSSION

The field of cell microencapsulation is improving and optimizing its potential for the treatment of an increasing number of diseases, thus, widening the horizons of its applicability. However, to address the new challenges, it is necessary to gain insight into the physicochemical and biological laws that surround and model this technology. As an interdisciplinary field, cell microencapsulation has to take advantage of the new engineering designs that provide novel particles of improved characteristics in a more controllable and scalable way. In this context, the present work describes how APA microcapsules can be reduced to 100 µm diameter particles using the *Flow Focusing System*, while maintaining all their functionality both in vitro and in vivo.

The capsule size is mainly governed by the focused liquid flow rate and the focusing air pressure, but characteristics of the fluids such as liquid density, liquid viscosity, liquid-air surface tension, employed polymer type and encapsulated cell density may have a significant effect on the final result. The dimensionless Weber (*We*), Reynolds (*Re*) and capillary numbers characterize the jet's behavior [32]. In particular, under the same liquid flow rate and air pressure, higher viscosities (smaller *Re*) result in larger jet diameters. An additional parameter is the Reynolds number Re_D of the nozzle tip associated to the focusing air. As a reduction in the nozzle tip diameter decreases Re_D and makes the air flow more laminar, we keep the nozzle diameter small enough to avoid subjecting the jet, and consequently the cells, to a turbulent flow (high Re_D). Besides, the smaller the focused flow rate compatible with the presence of a steady jet (i.e. *We* should be above a critical value of the order unity [32,33]), the smaller the jet diameter and the more laminar the jet flow are. Thus, for the present study we set the flow rate as low as 2 mL/h, reducing the risk of clogging the nozzle tip, too. *We* represents the ratio of the focused fluid inertia over the surface tension forces on the jet. To ensure a good monodispersity in generated beads, a relatively low *We* is needed. To this end, it must be $1 < We < 40$ to avoid non-symetric or turbulent breakup [23]. We noticed that the focusing air pressure had to be increased with the cell load to keep the jet size, pointing to a possible increase in the effective liquid viscosity with cell load which demands an increase of the air pressure to compensate it. Furthermore, any trace of bubbles was carefully eliminated from the pre-gelled solution for a correct behavior of the *Flow Focusing System.*

Besides, once the beads are formed, the further coating processes are also important at this particle size level. The washing steps were moved from PBS to 1% manitol

solution in order to avoid shrunk microcapsules. The amount of PLL bound to the capsule surface depends on the amount of the negative charges, which is especially evident in non-homogeneous beads, where charge density is mainly concentrated in the surface. The use of a saline solution elicits the dissolution of the gelled matrix by exchange of the Ca^{++} ions that form the known "egg box" between the mannuronic residues. This permits negative charges to be more accessible for the PLL to bind to, which eventually causes the microcapsule collapse. This phenomenon was described before and more specifically by B.L. Strand *et al*., who proposed the use of iso-osmotic manitol solution instead of PBS [34].

After optimizing all the technical issues required to produce highly monodisperse 100 µm diameter APA microcapsules (Fig 1), the next concern was to optimize the cell load within the particles. It is known that as the bead size is reduced, the probabilities to obtain empty capsules become higher. Since the number of cells enclosed into each particle is ruled by Poissonian statistics on the basis of the initial cell load in the pre-gelled solution, the probabilities of empty capsules for each cell load may be easily estimated after a simple calculation of the expected average of cells per capsule (Fig 2 A). In the practice, it has been observed that the number of empty capsules for each cell load fitted quite well with those estimated by the mathematical model (Fig 2 B-C).

However, and even if the encapsulation process is maintained in physiological and mild conditions, a slight cell viability loss (10%) causes a displacement in the distribution curve, translating into a higher number of non functional capsules (capsules without a single living cell inside), which have been considered "Dead Capsules" by the authors in the present work. Thus, this group of non-functional capsules would be roughly formed by the sum of empty capsules and capsules entrapping a single cell. As $2x10^6$ cells/mL and $5x10^6$ cells/mL loads give rise to a vast majority of capsules bearing from 0 to 2 cells per capsule, they are more susceptible to accumulate non-functional capsules upon minimal cell viability loss (Fig 2 B-C). Therefore, in order to optimize the encapsulation yield and to ensure the total functionality of the capsules, it is strongly convinient to use cell loads equal or higher than $10x10^6$ cells/mL. In fact, this initial cell load may be very close to the optimum one, since higher cell loads may give rise to several problems during the encapsulation process.

There are additional issues that must be taken into account. Reducing particle size results in a better relation surface/volume, but at the same time encapsulated cells are more exposed to the PLL coat, which is known to be immunogenic and may compromise cell viability [35,36]. Moreover, since alginate beads are not homogenously gelled, a stiffness gradient that decreases from the surface to the core, is formed in the particle. This means that most of the cells enclosed within the typical 450 µm APA capsules reside in a softer environment than those living within 100 µm ones, which might hinder cell proliferation due to the nanoporous nature of the matrices [37]. In addition, due to all the physicochemical changes that may arise, it is of the great importance to ensure that permeability will not become a new limiting factor.

In order to clarify whether all these points affect cell viability, three different capsule batches were compared. Liquid core APA capsules avoided the matrix stiffness problem while uncoated ones were used to discard either permeability or PLL cytotoxicity concerns. No differences in metabolic activity were found between the 3 groups during 31 days of the in vitro study (Fig 3 A). Interestingly, the APA group demonstrated a superior behavior, what it seems to rule out all the potential negative effects considered above.

KDR secretion was measured in parallel with metabolic activity assays (Fig 3 B). Results show that metabolic activity and KDR secretion do not correlate at the

beginning of the experiment but they do after day 10. Authors hypothesize that such phenomenon could be given as a result of a possible stabilization phase, where cells adapt their metabolism and functionality to the new environment. Uncoated group sustained higher levels of KDR secretion during the whole assay, but the differences were progressively reduced until being non significant by the last 2 weeks. The molecular weight of the soluble KDR is about 80 kD, which is close to the cut off value of APA microcapsules reported in the literature [38]. It may be reasonable that KDR secretion may be slightly more hindered in coated microcapsules compared to uncoated ones. In any case, from day 24 onwards, the greater metabolic activity shown by APA microcapsules seemed to compensate the diffusion differences with respect to the uncoated group as no statistical differences were obtained. Further permeability characterization will provide detailed information about this issue. Finally, when assayed encapsulated cells with the LIVE/DEAD cell viability kit, it was seen that in spite of the differences observed, all the groups maintained a good and sustained viability during the experiment (Fig 3 C).

When cell proliferation rate within APA and liquid core capsules was compared, both groups showed active BrdU uptake that even increased from the beginning to the end of the experiment (Fig 4). All these *in vitro* data are in agreement with those reported by our group [39] and suggest that matrix stiffness and particle stability may play a critical role for the cell welfare. Therefore, all the hypothesized drawbacks for APA microcapsules even at this size were discarded, confirming its suitability as microcapsule design.

Beyond *in vitro* analysis, *in vivo* intravitreous administration procedure also needs further optimization. Considering that the crystalline lens occupies a large part of ocular cavity in rats, we decided to assay a total dose as reduced as 10 µL, in order to avoid eye damage. This volume dose was translated into 6781 ± 1327 capsules, loading the average number of 5 cells per capsule (oscillating according to Poisson's Distribution) when administered through a 25G needle (Fig 5 A-C). This needle diameter gauge was found as the optimum one, small enough not to injure the eye but still able to administer the maximum capsule load with the lowest variability. The correct delivery of capsules in the eye cavity was confirmed by retinography minutes after administration (Fig 5 D).

Intravitreous space represents one of the immunoprivileged zones of the organism, but at the same time it offers an uncommon hypoxic environment to the enclosed cells [40]. Hence, in order to ensure the correct adaptation of the implant to the vitreous humor environment, the viability of the encapsulated cells was monitored over the following 3 weeks. During this time, a strong signal was obtained, confirming the viability of the enclosed cells (Fig 6).

In summary, this study represents a new milestone for the field of cell microencapsulation and the start point to explore new administration ways. Further investigation will be needed to find the most suitable cell line to encapsulate in each particular case and prove its efficacy in the treatment of ophthalmic diseases. Moreover, these reduced microparticles may be appropriate to reach difficult targets so far, such as those related with the eye and the Central Nervous System.

CONCLUSION

The present study covers a comprehensive technological development introducing the *Flow Focusing System* as a promising technique to obtain highly monodisperse 100 µm APA microcapsules. Indeed, this work reinforces the suitability of APA capsules even at this particular size. These preliminary results open the door to further investigations, where the effectiveness of this technology might be tested in a retinopathy model.

ACKNOWLEDGMENTS

E. Santos thanks the “Gobierno Vasco (Departamento de Educación, Universidades e Investigación)” for receiving a PhD fellowship. This study is partially financed by the “Ministerio de Ciencia e Innovación (PET-2008-330-01)”. Alfonso Gañán is thanked for valuable comments.

REFERENCES

[1] P. Aebischer, J. Ridet. Recombinant proteins for neurodegenerative diseases: the delivery issue. Trends Neurosci. 24 (2001) 533-40.

[2] M.S. Shoichet, S.R. Winn. Cell delivery to the central nervous system. Adv. Drug. Deliv. Rev. 42(2000) 81-102.

[3] Orive G, Hernández RM, Gascón AR, Calafiore R, Chang TM, De Vos P, Hortelano G, Hunkeler D, Lacík I, Shapiro AM, Pedraz JL. Cell encapsulation: promise and progress. Nat. Med. 9 (2003) 104-7.

[4] G.J. Lim, S. Zare, M. Van Dyke, A. Atala. Cell microencapsulation. Adv. Exp. Med. Biol. 670 (2010) 126-36.

[5] A. Murua, A. Portero, G. Orive, R.M. Hernández, M. de Castro, J.L. Pedraz. Cell microencapsulation technology: towards clinical application. J. Control Release. 132 (2008) 76-83.

[6] B. Salmons, M. Löhr, W.H. Günzburg. Treatment of inoperable pancreatic carcinoma using a cell-based local chemotherapy: results of a phase I/II clinical trial. J. Gastroenterol. 38 Suppl 15 (2003) 78-84.

[7] J. Bloch, A.C. Bachoud-Lévi, N. Déglon, J.P. Lefaucheur, L. Winkel, S. Palfi, J.P. Nguyen, C. Bourdet, V. Gaura, P. Remy, P. Brugières, M.F. Boisse, S. Baudic, P. Cesaro, P. Hantraye, P. Aebischer, M. Peschanski. Neuroprotective gene therapy for Huntington's disease, using polymer-encapsulated cells engineered to secrete human ciliary neurotrophic factor: results of a phase I study. Hum. Gene. Ther. 15 (2004) 968-75.

[8] R. Calafiore, G. Basta, G. Luca, A. Lemmi, L. Racanicchi, F. Mancuso, M.P. Montanucci, P. Brunetti. Standard technical procedures for microencapsulation of human islets for graft into nonimmunosuppressed patients with type 1 diabetes mellitus. Transplant Proc. 38 (2006) 1156-7.

[9] P.A. Sieving, R.C. Caruso, W. Tao, H.R. Coleman, D.J. Thompson, K.R. Fullmer, R.A. Bush. Ciliary neurotrophic factor (CNTF) for human retinal degeneration: phase I trial of CNTF delivered by encapsulated cell intraocular implants. Proc. Natl. Acad. Sci. U.S.A. 103(2006) 3896-901.

[10] C. Spuch, D. Antequera, A. Portero, G. Orive, R.M. Hernández, J.A. Molina, F. Bermejo-Pareja, J.L. Pedraz, E. Carro. The effect of encapsulated VEGF-secreting cells on brain amyloid load and behavioral impairment in a mouse model of Alzheimer's disease. Biomaterials. 31 (2010) 5608-18.

[11] S. Sugiura, T. Oda , Y. Aoyagi, R. Matsuo, T. Enomoto, K. Matsumoto, T. Nakamura, M. Satake, A. Ochiai, N. Ohkohchi, M. Nakajima. Microfabricated airflow nozzle for microencapsulation of living cells into 150 micrometer microcapsules. Biomed. Microdevices. 9 (2007) 91-9.

[12] R. Robitaille, J.F. Pariseau, F.A. Leblond, M. Lamoureux, Y. Lepage, J.P. Hallé. Studies on small (<350 microm) alginate-poly-L-lysine microcapsules. III. Biocompatibility Of smaller versus standard microcapsules. J. Biomed. Mater. Res. 44(1999) 116-20.

[13] J.T. Wilson , E.L. Chaikof , Challenges and emerging technologies in the immunoisolation of cells and tissues. Adv. Drug. Deliv. Rev. 60 (2008)124-45.

[14] S. Sakai, K. Kawakami. Development of subsieve-size capsules and application to cell therapy. Adv. Exp. Med. Biol. 670 (2010) 22-30.

[15] J. Xie, C.H. Wang. Electrospray in the dripping mode for cell microencapsulation. J. Colloid. Interface. Sci. 312 (2007) 247-55.

[16] V.T. Tran, J.P. Benoît, M.C. Venier-Julienne. Why and how to prepare biodegradable, monodispersed, polymeric microparticles in the field of pharmacy? Int. J. Pharm. 407 (2011) 1-11.
[17] C. Schwinger, A. Klemenz, K. Busse, J.Kressler. Encapsulation of living cells with polymeric systems. Macromol. Symp. 210 (2004) 493-99.
[18] J.M. Rabanel, X. Banquy, H. Zouaoui, M. Mokhtar, P. Hildgen. Progress technology in microencapsulation methods for cell therapy. Biotechnol. Prog. 25 (2009) 946-63.
[19] L.S Kontturi, M. Yliperttula, P. Toivanen, A. Määttä, A.M. Määttä, A. Urtti. A laboratory-scale device for the straightforward production of uniform, small sized cell microcapsules with long-term cell viability. J. Control Release. (2011) doi:10.1016/j.jconrel.2011.03.005.
[20] C.J. Ross, P.L. Chang. Development of small alginate microcapsules for recombinant gene product delivery to the rodent brain. J. Biomater. Sci. Polym. Ed. 13 (2002) 953-62.
[21] J. Hong, A.J. deMello, S.N. Jayasinghe. Bio-electrospraying and droplet-based microfluidics: control of cell numbers within living residues. Biomed. Mater. 5 (2010) 21001.
[22] A.M. Gañán-Calvo, J.M. Gordillo. Perfectly Monodisperse Microbubbling by Capillary Flow Focusing. Phys. Rev. Lett. 87 (2001) 274501.
[23] L. Martín-Banderas, M. Flores-Mosquera, P. Riesco-Chueca, A. Rodríguez-Gil, A. Cebolla, S. Chávez, A.M. Gañán-Calvo. Flow Focusing: a versatile technology to produce size-controlled and specific-morphology microparticles. Small 1 (2005) 688-92.
[24] J.Z. Nowak. Age-related macular degeneration (AMD): pathogenesis and therapy. Pharmacological reports : 58 (2006) 353-363.
[25] N. Kwak , N. Okamoto, J.M. Wood, P.A. Campochiaro. VEGF is major stimulator in model of choroidal neovascularization. Invest Ophthalmol Vis Sci. 41(2000) 3158-3164.
[26] N.M. Bressler. Early detection and treatment of neovascular age-related macular degeneration. J Am Board Fam Pract. 15 (2002) 142-152.
[27] C.A Augood, J.R. Vingerling, P.T. de Jong, U. Chakravarthy, J. Seland, G. Soubrane, L. Tomazzoli, F. Topouzis, G. Bentham, M. Rahu, J. Vioque, I.S. Young, A.E. Fletcher. Prevalence of age-related maculopathy in older Europeans: the European Eye Study (EUREYE). Arch Ophthalmol. 124 (2006) 529-535.
[28] G.C. Brown, M.M. Brown, S. Sharma, J.D. Stein, Z. Roth, J. Campanella, G.R. Beauchamp. The burden of age-related macular degeneration: a value-based medicine analysis. Trans Am Ophthalmol Soc. 103 (2005) 173-184
[29] V. Ponomarev, M. Doubrovin, I. Serganova, J. Vider, A. Shavrin, T. Beresten, A. Ivanova, L. Ageyeva, V. Tourkova, J. Balatoni, W. Bornmann, R. Blasberg, J. Gelovani Tjuvajev, A novel triple-modality reporter gene for whole-body fluorescent, bioluminescent, and nuclear noninvasive imaging. Eur. J. Nucl. Med. Mol. I. 31 (2004) 740-751.
[30] R. Catena, E. Santos, G. Orive, R.M. Hernández, J.L. Pedraz, A. Calvo. Improvement of the monitoring and biosafety of encapsulated cells using the SFGNESTGL triple reporter system. J. Control Release. 146 (2010) 93-8.
[31] F. Lim, A.M. Sun. Microencapsulated islets as bioartificial endocrine pancreas. Science. 210 (1980) 908-10.

[32] A.M. Gañán-Calvo, J.M. Montanero. Revision of capillary cone-jet physics: electrospray and flow focusing. Phys. Rev. E. Stat. Nonlin. Soft. Matter. Phys. 79 (6 Pt 2) (2009) 066305.
[33] J.M. Montanero, N. Rebollo-Muñoz, M.A. Herrada, A.M. Gañán-Calvo. Global stability of the focusing effect of fluid jet flows. Phys. Rev. E. 83 (3 Pt2) (2011) 036309.
[34] B.L. Strand, O. Gåserød, B. Kulseng, T. Espevik, G. Skjåk-Baek. Alginate-polylysine-alginate microcapsules: effect of size reduction on capsule properties. J. Microencapsul. 19 (2002) 615-30.
[35] S. Ponce, G. Orive, R. Hernández, A.R. Gascón, J.L. Pedraz, B.J. de Haan, M.M. Faas, H.J. Mathieu, P. de Vos. Chemistry and the biological response against immunoisolating alginate-polycation capsules of different composition. Biomaterials. 27 (2006) 4831-9.
[36] G. Orive, S.K. Tam, J.L. Pedraz, J.P. Hallé. Biocompatibility of alginate-poly-L-lysine microcapsules for cell therapy. Biomaterials. 27 (2006) 3691-700.
[37] E. Hill, T. Boontheekul, D.J. Mooney. Designing scaffolds to enhance transplanted myoblast survival and migration. Tissue Eng. 12 (2006) 1295-304.
[38] A. Leung, L.K. Nielsen, M. Trau, N.E. Timmins. Tissue transplantation by stealth—Coherent alginate microcapsules for immunoisolation. Biochem. Eng. J. 48 (2010) 337-47.
[39] G. Orive, R.M. Hernández, A.R. Gascón, M. Igartua, J.L. Pedraz. Survival of different cell lines in alginate-agarose microcapsules. Eur. J. Pharm. Sci. 18 (2003) 23-30.
[40] J.Y. Niederkorn. See no evil, hear no evil, do no evil: the lessons of immune privilege. Nat. Immunol. 7 (2006) 354-9.

FIGURE LEGENDS

Fig 1. Morphology of C_2C_{12}-TGL-KDR cells encapsulated within 100µm APA microcapsules. Optical microscopy at different maginifications. Scale bars are presented for each picture.

Fig 2. Optimization of cell load. (**A**) Mathematical model of Poisson distribution for cells encapsulated within 100 µm APA microcapsules. (**B-C)** Encapsulation yields obtained for the different cell loads. Encapsulated cells were dyed with the LIVE/DEAD kit. Microcapsules showing no single living cell (green) were considered as Dead Capsules. Corresponding results are represented in the histogram (**B**) and fluorescence microcagraphies (**C**). Error bars represent the standar desviation in the histogram. Scale bar = 100 µm in pictures.

Fig 3. *In vitro* evaluation of the microcapsules to evaluate any possible detriment of functionality due to the size reduction. APA microcapsules were contrasted against liquid core group, in order to rule out differences arising from matrix stiffness, and uncoated group, which avoids both permeability limitations and overexposure to poly-L-lysine. (**A**) Metabolic activity of encapsulated cells. n=7 (**B**) KDR secretion. n=3 (in duplicate). (**C**) Fluorescence micrographies of encapsulated cells obtained with the LIVE/DEAD kit. Scale bar represents 100 µm. Data are shown as mean ± S.D. (error bars) and either statistical significances (**$p<0.01$) or no-significances (N.S.).

Fig 4. *In vitro* BrdU uptake of enclosed cells. APA group was compared with liquid core group in order to assess the influence of matrix stiffness in cell proliferation. n=5. Both groups demonstrated active proliferation comparing with control groups. At day 35 APA capsules showed higher proliferation activity, which resulted statistically significative beside results obtained by the same group at day 10 and liquid core group at day 35. Data represent the mean ± S.D. (error bars). Statistical significances are shown as (*$p<0.05$) or (**$p<0.01$).

Fig 5. Optimization of administration protocol. (**A**) The histogram express the mean ± S.D. (error bars) of the number of microcapsules per 10 µL administered by needles of different gauge and (**B**) shows the variability (CV) obtained with each needle diameter. (**C**) 10 µL microcapsule dose dyed with membrane blue. (**D**) Retinography taken minutes after administration of membrane blue dyed microcapsules.

Fig 6. Luminometries of encapsulated cells during 3 consecutive weeks. Treated eyes glowed strongly in all the rats. Figure shows a different rat as the representative image of the group (n=3) for each monitorized week, so that all the rats can be displayed.